# CHAPTER IV

# RESULTS AND DISCUSSION

## 4.1 Model Studies

The major objective of this part is to form crosslinked network at the "interphase" between squalene (a natural rubber model) with vinyl-containing silicon oxide surfaces (a flat surface model for silica) and to study the effect of the silane reagent and the catalyst on the thickness of the crosslinked network. Contact Angle measurement, ellipsometry and x-ray photoelectron spectroscopy (XPS) were used as major characterization techniques.

### 4.1.1 Preparation of Vinyl-containing Silicon Oxide Surfaces

Reactions between silicon oxide surfaces containing silanol groups and vinyldimethylchlorosilane were carried out to determine the optimized condition that can give the maximum bonding density which can be characterized by contact angle measurements.

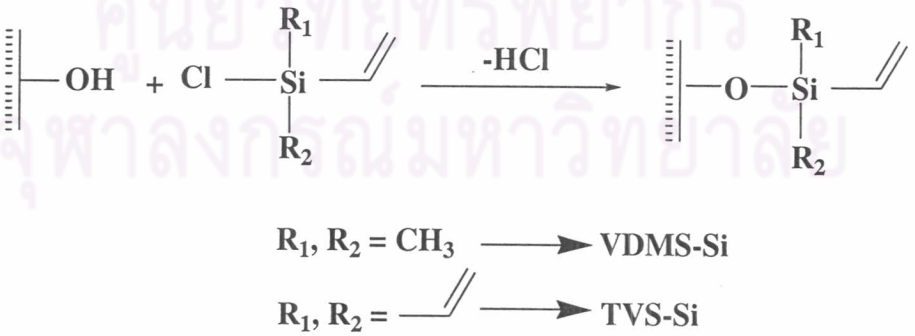


**Scheme 4.1** Reaction between a silicon oxide surface with vinyl-containing silane reagents.

Both water and hexadecane contact angle data (see Table 4.1) suggested that hydrophobization has relatively reached its maximum within the first 24h of the reaction performed in toluene solution in which diisopropylethylamine (DIEA) was added. Elevated temperature does not seem to influence the extent of reaction. Greater water contact angle hysteresis implied the less densed modified layer was formed in the vapor phase reaction. The speculation was also confirmed by lower hexadecane contact angle due to the ability of hexadecane to penetrate the incomplete silane monolayer and interact with surface silanols. This indicates that DIEA can truly magnify the rate of reaction and has a stronger impact on the extent of reaction than the temperature does for this specific silane reagent. An addition of tertiary amine has been proven not only to neutralize hydrogen chloride generated during the substitution reaction but also to enhance chemisorption of the silane reagent at the toluene/silicon interface. Hydrogen bonding between tertiary amine (DIEA in this case) and hydroxyl groups of silanol promotes the substitution of silane [27]. This observation, however, does not agree with the work reported earlier by Fadeev and McCarthy [24]. They found denser silanized surfaces generated when the reaction proceeded in the vapor phase without base. This can be described as a result of vinyl groups being sensitive to other side reactions such as oxidation, self-crosslinking at elevated temperature. Unlike its saturated analog, the ability to pack molecules of vinyl-containing silanes by themselves is not sufficient enough in the absence of solvent. Both hypotheses tend to deteriorate the reaction progress. It thus becomes necessary to incorporate DIEA into the reaction to obtain fully functionalized surface. To minimize the possibility of side reactions, the reaction in

toluene at room temperature for 48h in the presence of DIEA was chosen as an optimized condition.

The optimized condition for surface silanization by VDMS was confirmed by a full kinetic study in toluene solution at ambient temperature as displayed in Figure 4.1. As monitored by water contact angle measurements, it seems that surface silanization by TVS also reached its maximum density after 48h. According to the result from ellipsometric analysis, a monolayer of vinyldimethylsilyl (VDMS) and trivinylsilyl (TVS) groups was readily formed with a thickness of 7 and 12 Å on top of the silicon oxide layer (23 Å). Upon the formation of vinyldimethylsilyl monolayer, it is obvious that the surface hydrophobicity was potentially improved. Water contact angles of the vinyl-functionalized surface increased from 46°/31° of the cleaned silicon oxide to 94°/88° and 94°/81° of the silicon oxide containing vinyldimethylsilyl groups (VDMS-Si) and trivinylsilyl groups (TVS-Si) using the same optimized condition, respectively. This enhanced hydrophobicity should also accommodate the compatibility between silica and natural rubber to some extent.

**Table 4.1** Water and hexadecane contact angle data of silicon oxide surfaces after reaction with vinyldimethylchlorosilane.

| **Condition** | **Temperature (°C)** | **Reaction time (h)** | **$\theta_A/\theta_R$(°) of water** | **$\theta_A/\theta_R$(°) of hexadecane** |
|---|---|---|---|---|
| In toluene with DIEA | Ambient temperature | 24 | 93/84 | 33/29 |
| | | 48 | 94/88 | 32/27 |
| | | 72 | 93/87 | 29/25 |
| | 70 | 24 | 93/86 | 32/27 |
| In vapor phase without DIEA | 70 | 24 | 93/76 | 21/15 |
| | | 48 | 90/77 | 22/14 |

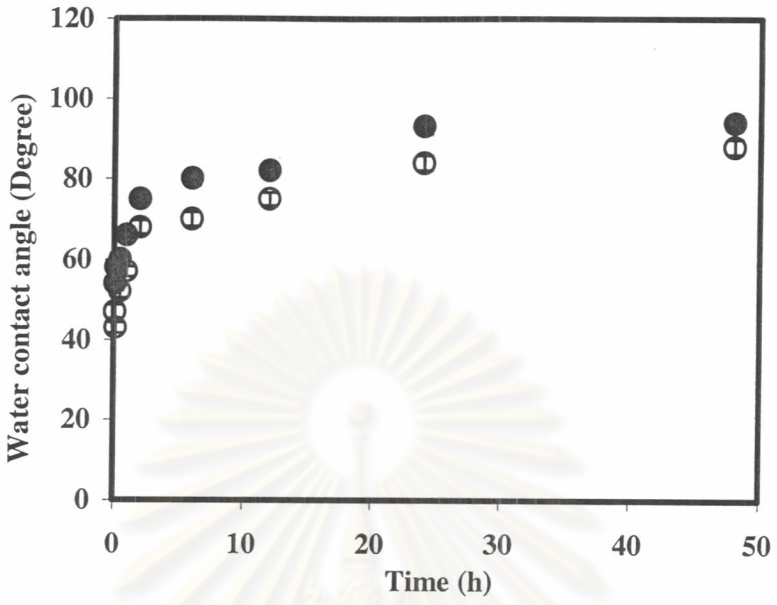


**Figure 4.1** Water contact angle data of silicon oxide surfaces after a reaction with vinyldimethylchlorosilane as a function of reaction time : advancing contact angle (●); receding contact angle (○).

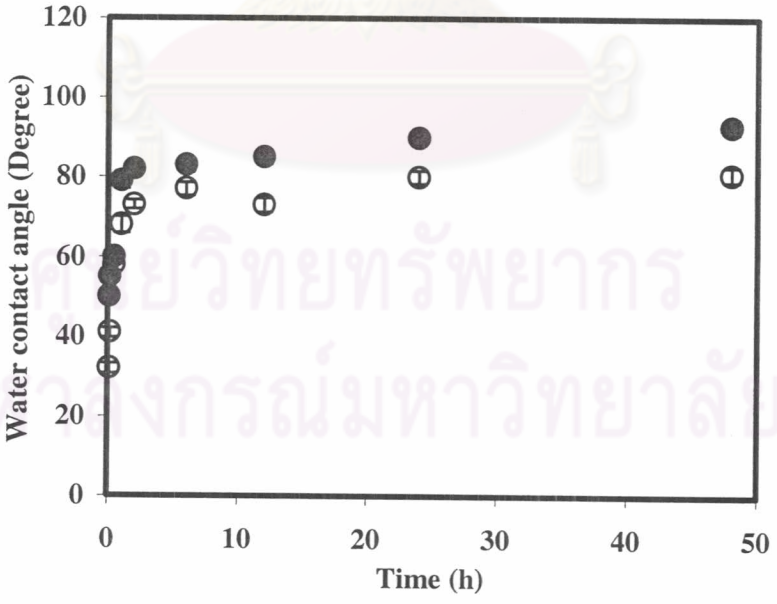


**Figure 4.2** Water contact angle data of silicon oxide surfaces after a reaction with trivinylchlorosilane as a function of reaction time: advancing contact angle (●); receding contact angle (○).

The presence of vinyl groups on silicon oxide surface after surface treatment was confirmed by the detection of 2.89% and 7.40% bromine on silicon oxide surfaces containing vinyldimethylsilyl groups (VDMS-Si) and trivinylsilyl groups (TVS-Si), respectively after bromination. The signals $Br_{3d}$ (at 95-165 eV) in Table 4.2 indicated that TVS-Si has approximately 2.6 times of vinyl groups on the surface as compared to ones on VDMS-Si. We did not intend to quantify the vinyl group density on the silicon surfaces after bromination due to the fact that bromine element is somewhat labile under prolonged exposure to x-ray. As a result, only qualitative data is available.

**Table 4.2** XPS atomic composition data of VDMS-Si and TVS-Si after bromination.

| Surface | XPS atomic composition (%) | | | |
|---|---|---|---|---|
| | Si | C | O | Br |
| VDMS-Si after bromination | 41.49 | 22.42 | 33.20 | 2.89 |
| TVS-Si after bromination | 30.15 | 34.30 | 28.15 | 7.40 |

### 4.1.2 Reaction of Vinyl-containing Surfaces with Squalene and Squalane

Initially, reactions were carried out using AIBN, a common radical initiator for radical polymerization and crosslinking. Overall XPS atomic composition and layer thickness of VDMS-Si before and after reacted with squalene (SqE) and its saturated analog (SqA) are summarized in Table 4.3. After the reaction with SqA, %C (from 15° take-off angle data) increased from 27.55% of VDMS-Si to 36.49% after 2.5h and continued increasing to 42.07% after 5h. The same trend was observed

from 75° take-off angle data. It should be noted that the data obtained from 15° and 75° take-off angles ($\theta_T$) project the information from the sampling depth of approximately 10 Å and 40 Å, respectively. Eventhough %C became higher using a longer reaction time, the attenuation of %Si has reached the minimum after 2.5 h and remained relatively unchanged for up to 5h. This suggests that crosslinking process within that interfacial layer still continued even after 2.5h to generate a denser layer without significantly affecting the thickness (retained at ~ 10 Å). A lack of %O increase implied that there was no sign of surface oxidation.

Atomic compositions of VDMS-Si surfaces before and after reactions with SqE were not distinguishable indicating there was no significant interfacial crosslinking taking place. We explain these unsuccessful reactions as a result of surface oxidation as evidenced from XPS data. Figure 4.3 shows XPS $C_{1s}$ and $O_{1s}$ spectra of VDMS-Si after a reaction with SqE. Interestingly, only 75° take-off angle spectra providing information at higher sampling depth showed peak splitting. The high binding energy peak in the range of 286-292 eV in $C_{1s}$ region presumably corresponded to carbons connected to electronegative element of oxygen in the form of O-C=O, C=O or C-O. The oxygen peak also evolved into two peaks; an origin oxygen peak from Si-O appearing at 534.5 eV while a new peak assigned to oxygen of C=O emerging at 537.0 eV. Relative intensities between the high binding energy peak and the low binding energy peak of $C_{1s}$ as well as $O_{1s}$ spectra were higher for the surface reacted for 5h implying the greater extent of oxidation.

**Table 4.3** XPS atomic composition of VDMS-Si before and after a reaction with SqA or SqE

| Sample | Time (h) | $\theta_T$ (°) | XPS atomic composition (%) | | |
|---|---|---|---|---|---|
| | | | C | O | Si |
| Cleaned Si-wafer | - | 15 | 23.42 | 47.42 | 29.16 |
| | | 75 | 6.85 | 39.11 | 54.04 |
| VDMS-Si | - | 15 | 27.55 | 40.27 | 32.17 |
| | | 75 | 11.69 | 37.91 | 50.40 |
| VDMS-Si AIBN, 70°C, SqA | 2.5 | 15 | 36.49 | 35.88 | 27.63 |
| | | 75 | 13.33 | 37.19 | 49.36 |
| | 5.0 | 15 | 42.07 | 30.45 | 27.48 |
| | | 75 | 15.23 | 36.56 | 48.21 |
| VDMS-Si AIBN, 70°C, SqE | 2.5 | 15 | 32.85 | 35.92 | 30.82 |
| | | 75 | 12.32 | 37.25 | 50.42 |
| | 5.0 | 15 | 33.96 | 35.21 | 30.83 |
| | | 75 | 12.81 | 37.55 | 49.64 |

In order to determine the effect of temperature, *t*-butyl peroxide was used as another radical initiator. Higher thermal decomposition temperature of *t*-butyl peroxide allows the reactions to be operated at higher temperature than 80 °C. Similar results were obtained. The interfacial layer formed at VDMS-Si/SqA (38 Å) was thicker than the one formed at VDMS-Si/SqE (9 Å). So attempts to prepare interfacial chemical bonding using two radical initiators (*t*-butyl peroxide and AIBN) were not successful due to non-selective radical process towards unsaturated moieties of squalene that lead to surface oxidation.

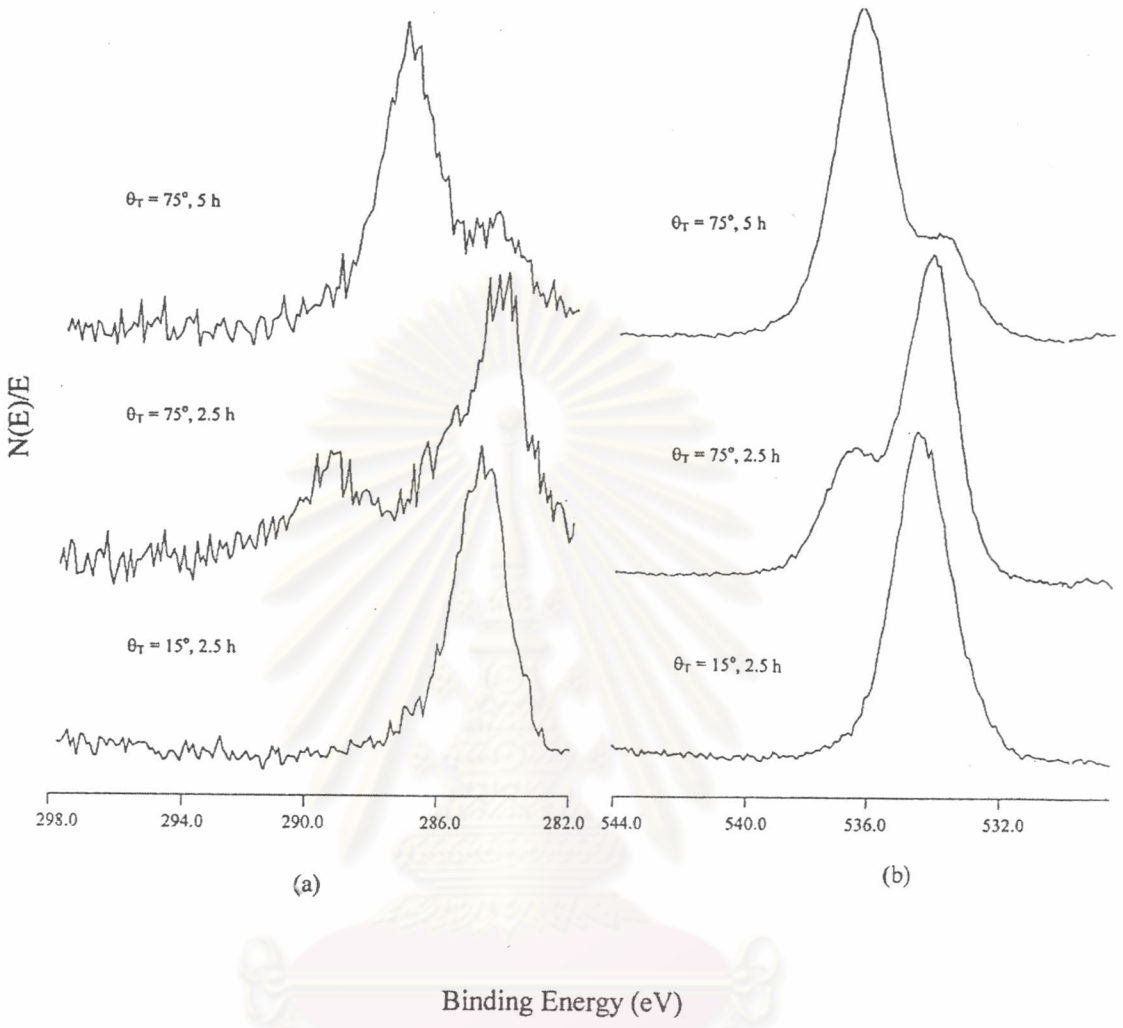


**Figure 4.3** XPS spectra of VDMS-Si after a reaction with SqE in the presence of AIBN (a) $C_{1s}$ spectra (b) $O_{1s}$ spectra.

To overcome the difficulties caused by SqE being sensitive to oxidation and the non-selectivity of radical process to unsaturated moieties of SqE, a radical initiator was then replaced by *p*-toluenesulfonic acid (*p*-TsOH). As expected, a cationic process can eliminate the problems and exhibited more desirable catalytic behavior. From Table 4.4, a crosslinked layer with the thickness of 21.8 Å (including the VDMS layer) was generated at the VDMS-Si/SqE interface after a reaction at 40 °C for 17 h. This data agreement well with XPS results: an attenuation of the Si

signal from the substrate as well as a significant increase of carbon concentration were evidenced. No sign of surface oxidation was detected. A lower extent of crosslinked network formation was observed when the reaction was carried out for 3h at higher temperature (70°C). Smaller extent of crosslinking at VDMS-Si/SqA interface was observed as compared to the ones occurred at VDMS-Si/SqE interface.

**Table 4.4** XPS atomic composition and layer thickness of VDMS-Si before and after reaction with SqA or SqE in the presence of *p*-TsOH.

| Sample | Time (h) | $\theta_T$ (°) | XPS atomic composition (%) | | | Layer Thickness[a] (Å) |
|---|---|---|---|---|---|---|
| | | | C | O | Si | |
| Cleaned silicon oxide | - | 15 | 23.42 | 47.42 | 29.16 | - |
| | | 75 | 6.85 | 39.11 | 54.04 | |
| VDMS-Si | - | 15 | 27.55 | 40.27 | 32.17 | 7.0 |
| | | 75 | 11.69 | 37.91 | 50.40 | |
| VDMS-Si, 40°C, SqA | 17.0 | 15 | 38.69 | 21.37 | 39.94 | 7.0 |
| | | 75 | 7.83 | 39.60 | 52.57 | |
| VDMS-Si, 40°C, SqE | 17.0 | 15 | 52.51 | 26.48 | 21.01 | 21.8 |
| | | 75 | 21.57 | 34.38 | 44.05 | |
| VDMS-Si, 70°C, SqA | 3.0 | 15 | 26.68 | 40.92 | 32.41 | 7.0 |
| | | 75 | - | - | - | |
| VDMS-Si, 70°C, SqE | 3.0 | 15 | 33.20 | 37.59 | 29.21 | 13.4 |
| | | 75 | - | - | - | |

[a] Layer thickness values include VDMS layer.

Figure 4.4 shows the effect of *p*-TsOH concentration on the layer thickness. The reaction was performed at 40°C for 6h using 10%SqE in toluene. The result

suggested that 5%(mol/mol) of *p*-TsOH/SqE was enough for the crosslinked layer to reach its maximum thickness for this particular condition. Based on the concept of bound rubber, we hypothesize that the thicker the crosslinked layer is, the more crosslinking is achieved considering that the cleaning procedure after reaction can efficiently remove the unreacted SqE from the surface. The effect of SqE concentration on the layer thickness was also determined in order to obtain the lowest concentration possible for further crosslinking studies. The information from Figure 4.5 implied that 35% SqE was sufficient to give the same crosslinked thickness as the one obtained when pure SqE was used. The effect of temperature on the progression of interfacial crosslinking formation can be explained from Figure 4.6. Considering the same range of reaction time, the higher the temperature was used, the thicker the thickness was achieved.

Eventhough the vinyl group density on TVS-Si is higher than one on VDMS-Si, kinetics of surface crosslinking of both substrates are quite similar. There is no significant impact of vinyl group density on the interfacial thickness. The data in Figure 4.7 indicated that the thickness of crosslinked layer increased linearly as a function of reaction time within the first 12h. The thickness tended to level off afterwards.

From practical point of view, the crosslinking reaction was also performed in the presence of sulfur, a conventional curing agent. A number of additives commonly used in rubber curing were added such as ZnO, TMTD. The reaction was carried out at 150°C, a temperature selected for curing silica-filled rubber composites. The data in Figure 4.8 suggested that the thickness of interfacial crosslinked layer marginally increased as a function of time. This outcome may be

regarded as a consequence of rapid curing at such a high temperature (150°C) particularly in the presence of sulfur along with accelerator and activator. In fact, this data corresponds well with the cure time later discussed in this chapter. Again, there is no evidence that indicates the difference between the thickness at VDMS-Si/SqE and TVS-Si/SqE interfaces.

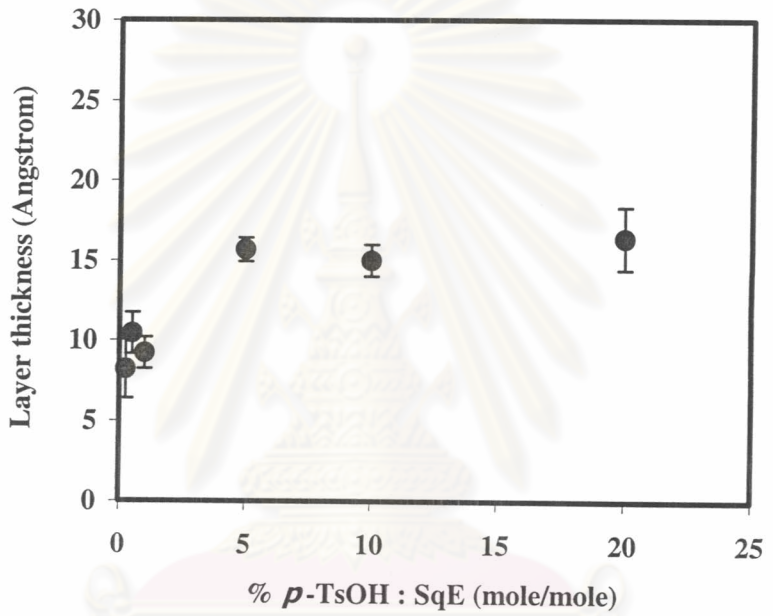


**Figure 4.4** The thickness of the crosslinked layer at VDMS-Si/SqE interface as a function of *p*-TsOH using SqE 10% (mole/mole), at 40 °C for 6h.

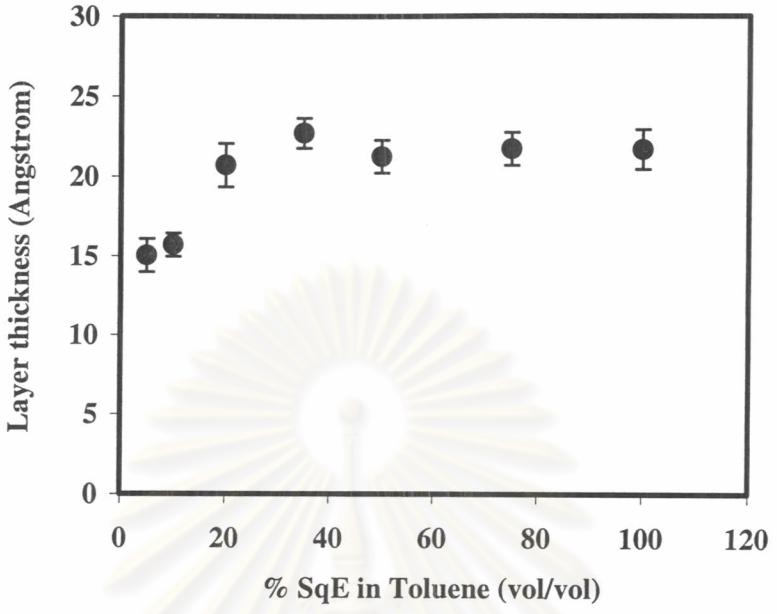


**Figure 4.5** The thickness of the crosslinked layer at VDMS-Si/SqE interface as a function of SqE using *p*- TsOH 5% (mole/mole) at 40°C for 6 h.

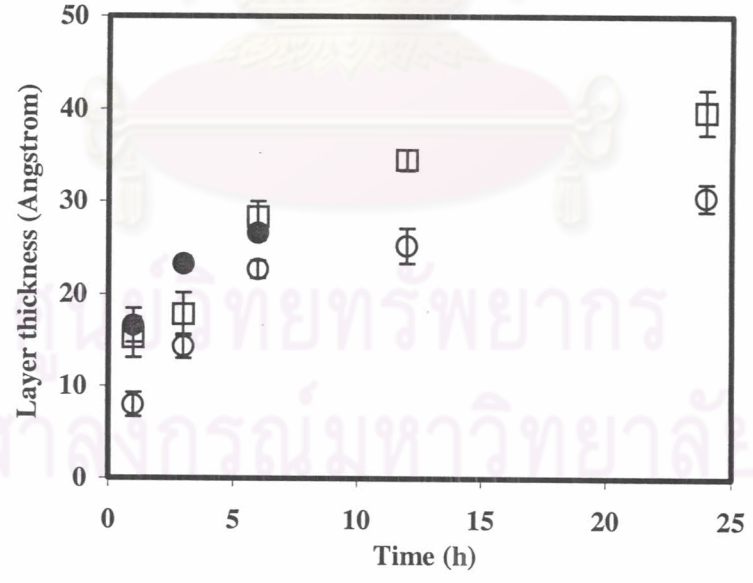


**Figure 4.6** The thickness of the crosslinked layer at VDMS-Si/SqE interface as a function of time using *p*- TsOH 5% (mole/mole) : 40°C (○), 70°C (□) and 150°C(●).

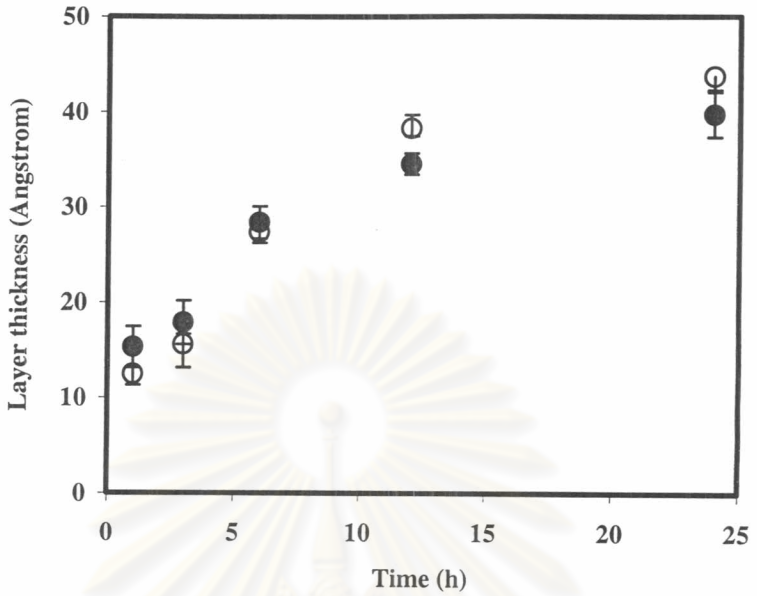


**Figure 4.7** The thickness of the crosslinked layer at VDMS-Si/SqE interface (●) and TVS-Si/SqE interface (○) using *p*- TsOH 5% (mole/mole) at 70°C.

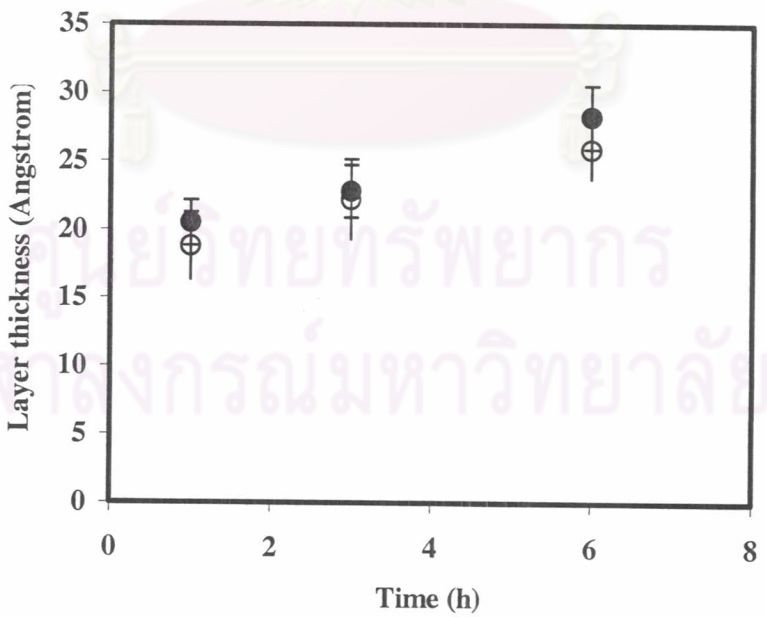


**Figure 4.8** The thickness of the crosslinked layer at VDMS-Si/SqE interface (●) and TVS-Si/SqE interface (○) in the presence of sulfur and other additives at 150°C.

## 4.2 Natural Rubber Composites Filled with Surface-treated Silica

### 4.2.1 Physical Properties of Surface-treated Silica

Silica and surface-treated silica were characterized prior to the determination of curing behavior and mechanical properties of silica-filled rubber composites. Physical properties of silica and surface-treated silica used in this study are given in Table 4.5. It was found that the mean agglomerate particle sizes of VDMS-Si and TVS-Si were smaller than the that of untreated silica indicating that an introduction of vinyl moieties on the silica surface helped reducing particle aggregation caused by attractive hydrogen bonding among silanol groups. The smaller the agglomerate particle size is, the better the particle distribution in the rubber matrix should be. However, the surface area as determined by BET method did not correspond well with the particle size. The fact that VDMS-Si has a relatively unchanged surface area as compared to the one of untreated silica may be explained as a result of heat treatment during BET measurement. According to the model studies, it has been demonstrated that the vinyl groups are quite sensitive to heat. It is thus possible that crosslinking at the surface of silica or between the silica particles may occur and led to the particle agglomeration and the reduction of surface area.

For TVS-Si, eventhough the surface area of TVS-Si is larger than the untreated silica, the magnitude of surface area increase did not correspond well with the particle size decrease. We suspect that heat affected the particle size and agglomeration in the similar manner as it did for the case of VDMS-Si. However, the particle agglomeration due to inter-particle crosslinking is dominated by repulsions among some uncrosslinked vinyl groups on the surface of TVS-Si. The density of

particle was influenced by the surface treatment only in the case of TVS-Si whose surface contains higher density of vinyl groups.

**Table 4.5** Physical properties of silica and surface treated silica.

| Fillers | Mean agglomerate particle (μm) | Surface area ($m^2/g$) | Density ($g/cm^3$) |
|---|---|---|---|
| Untreated silica | 94.04±1.38 | 127.76±0.44 | 2.69±0.0018 |
| VDMS-Si | 50.70±2.99 | 124.77±1.39 | 2.67±0.0009 |
| TVS-Si | 41.51±0.83 | 135.94±0.74 | 2.84±0.0015 |

### 4.2.2 Curing Behavior & Mooney Viscosity

STR 5L were compounded by conventional laboratory two-roll mill (160×320 mm) using sulfur as a vulcanizing agent. The rubber compound sheet was conditioned at 23°C for 24 h in a closed container before testing. Cure time ($t_{90}$) and scorch time at 150°C were obtained from Monsanto Rheometer MDR 2000 (moving die rheometer). Mooney viscosity (ML1+4@100°C) was measured by Monsanto automatic mooney viscometer (MV2000).

Figure 4.9 represents the effects of silica loading on cure time ($t_{90}$). The addition of surface treated silica (VDMS-Si or TVS-Si) reduced the cure time as compared to the untreated silica especially at high loading. For comparison, the curing of silica-filled rubber composite in the presence of Si-69 was also studied. The obtained information suggested that the surface treatment of silica can accelerate

the curing process as effectively as the conventional method of adding Si-69 as a coupling agent. According to Dannenberg, the cure enhancement is due to an improvement in filler dispersion in a rubber matrix by a silane coupling agent [28]. This statement should also be valid for the case of surface-treated silica. Figure 4.10 shows the effects of silica loading on scorch time. It can be seen that the scorch time of VDMS-Si-filled composite also decreased with increasing filler loading. Similar trend was observed for silica-filled composite mixed with Si-69. Using a similar filler loading, relatively longer scorch time was evidenced for the case of TVS-Si. This may be explained by the fact that the higher vinyl group density at the surface of TVS-Si required a longer period of time to begin the crosslinking.

Mooney viscosity of rubber composites filled with silica and surface-treated silica is shown in Figure 4.11. As expected, Mooney viscosity of rubber composites filled with untreated silica increases with increasing filler loading. Mooney viscosity of rubber composites filled with surface-treated silica or silica mixed with Si-69 varied in the range of 30-40 MV and was independent of filler loading. This characteristic is very useful from the processing perspective.

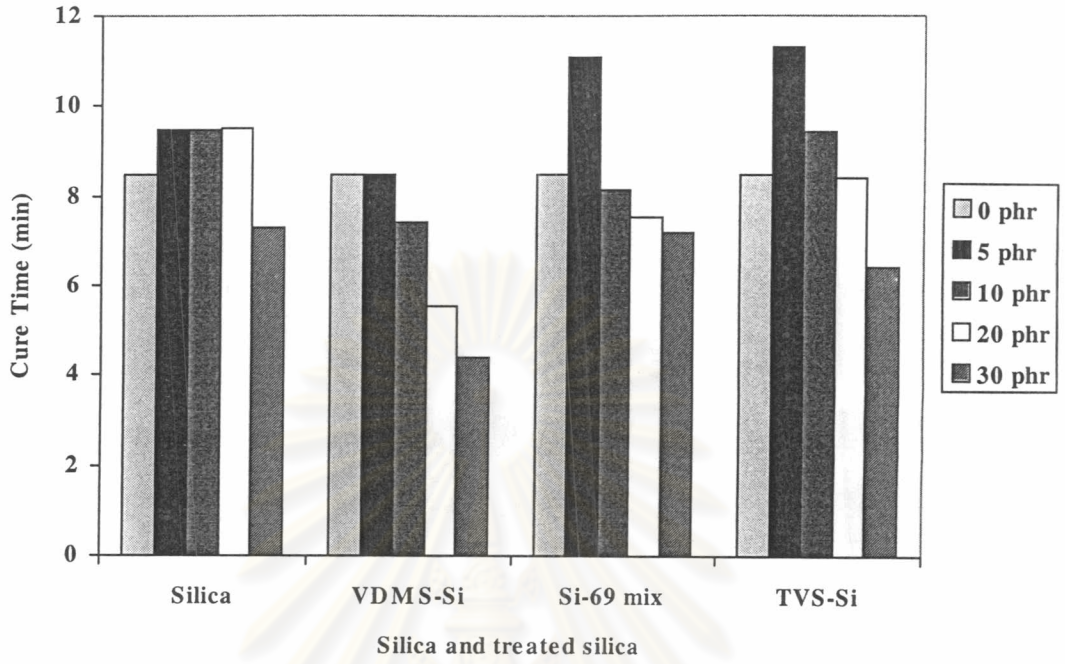


**Figure 4.9** Cure time ($t_{90}$) of natural rubber composites filled with silica.

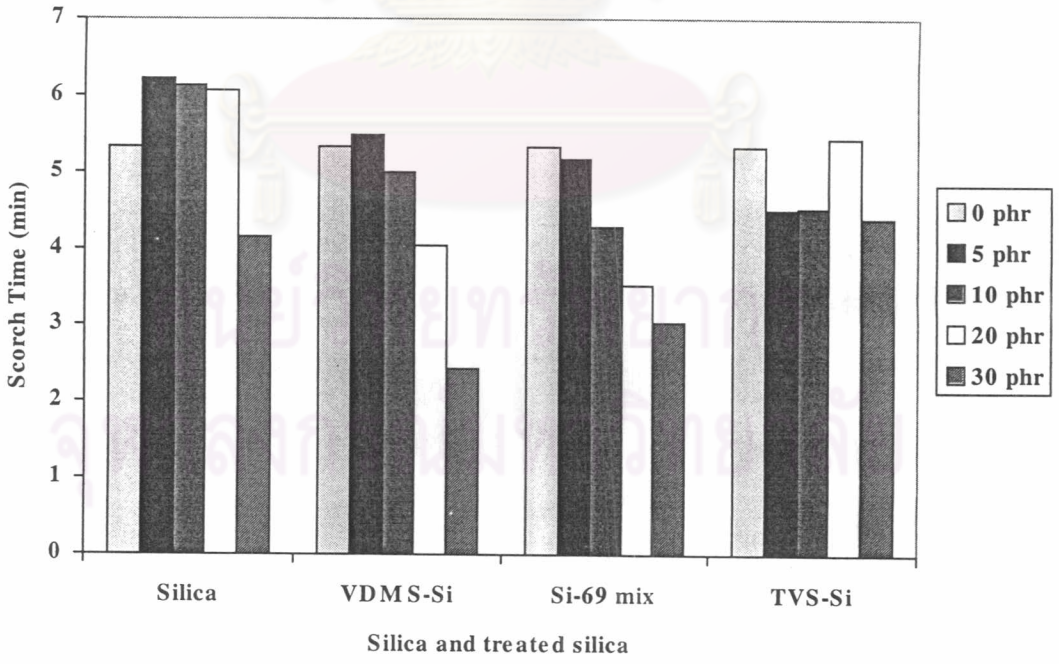


**Figure 4.10** Scorch time of natural rubber composites filled with silica.

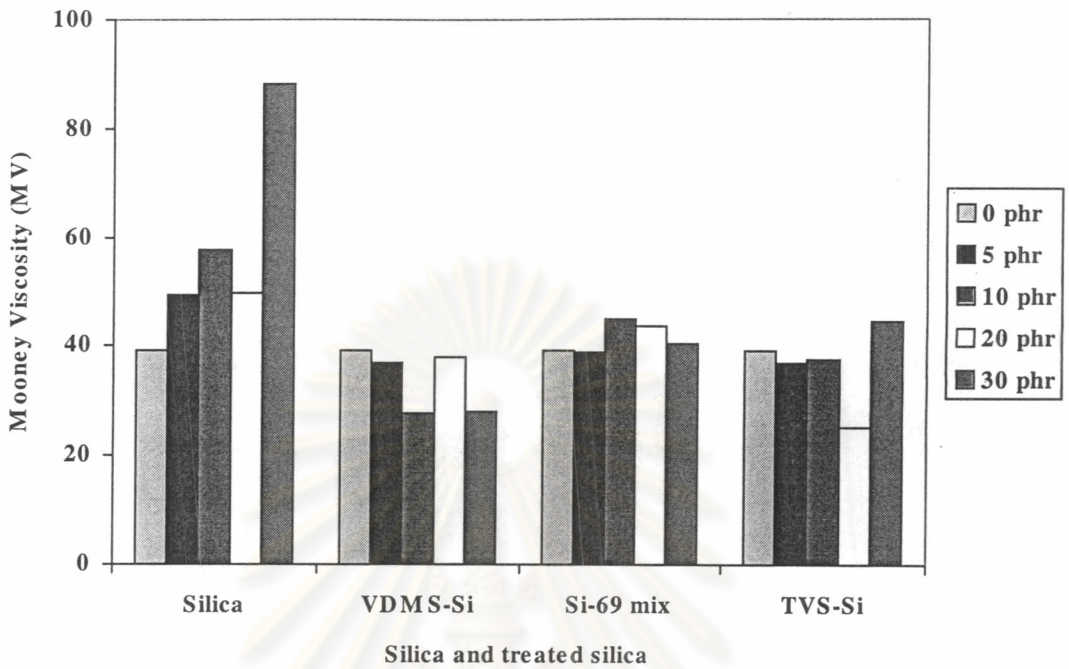


**Figure 4.11** Mooney viscosity of natural rubber composites filled with silica.

### 4.2.3 Mechanical Properties

Various rubber compounds were compressed in compression molding using hydraulic at 150°C according to their respective cure time ($t_{90}$) into sheets. Dumbbell and crescent test pieces were cut from the sheets for tensile and tear tests, respectively. Tensile and tear properties were determined by an Instron Tesing Machine, at 500 mm/min cross-head speed. The test for hardness was carried out using Shore Type A Durometer.

Figure 4.12 shows the effects of silica loading on tensile properties. It appeared that a composite with 30 phr VDMS-Si attained the highest tensile strength with a value close to the one having a similar loading of TVS-Si. The tensile strength of a rubber composite was elevated by an increase in the loading of VDMS-Si, TVS-

Si or untreated silica mixed with Si-69. VDMS-Si seems to be the most effective reinforced filler, particularly at a low loading (5 and 10 phr). While adverse effect was clearly seen in composites filled with TVS-Si or untreated silica mixing with Si-69. The result suggested that the successful reinforcement required a high filler loading (> 10 phr).

Although VDMS-Si seems to be the best filler from the result of tensile strength, the tear strength of the composite was not improved significantly in the presence of VDMS-Si filler (see Figure 4.13). From the data of tear strength, the addition of Si-69 appeared to be a more favorable method to increase the tear strength at high silica loading. TVS-Si is quite a competitive option due to its relatively high tear strength when as high as 30 phr was incorporated.

From Figure 4.14, it can be seen that the hardness of a composite was improved by an addition of VDMS-Si, TVS-Si or untreated silica mixing with Si-69. The higher filler loading was incorporated, the better hardness the composite had. The magnitude of hardness increase in all cases is almost indistinguishable using the same filler loading. Tensile modulus (M100) of all silica-filled composites was displayed in Figure 4.15. It should be noted that the same trend was observed for tensile modulus M300 (data is shown in Appendix). The composites filled with 10-30 phr of untreated silica and vulcanized in the presence of Si-69 show the highest tensile modulus as compared to the composites filled with the same loading of VDMS-Si or TVS-Si.

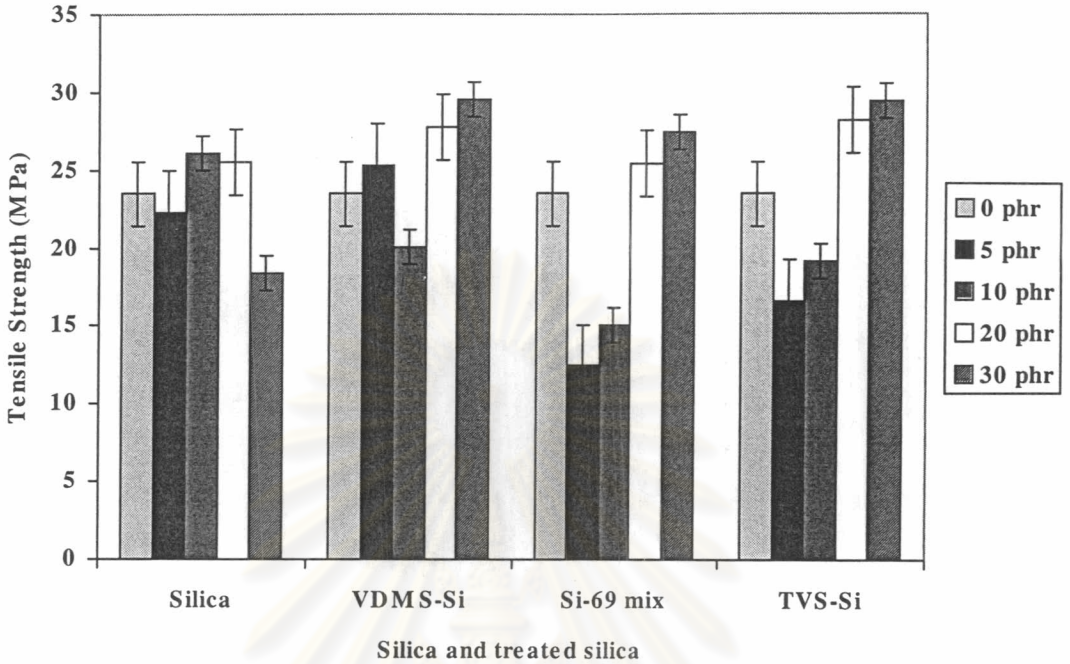


**Figure 4.12** Tensile strength of natural rubber composites filled with silica.

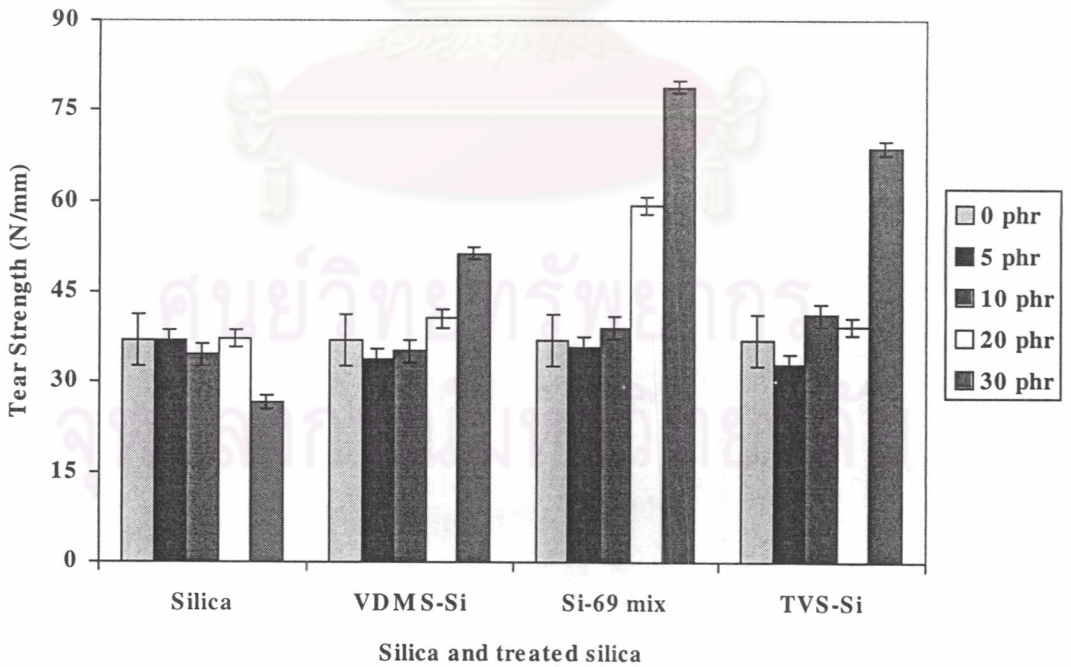


**Figure 4.13** Tear strength of natural rubber composites filled with silica.

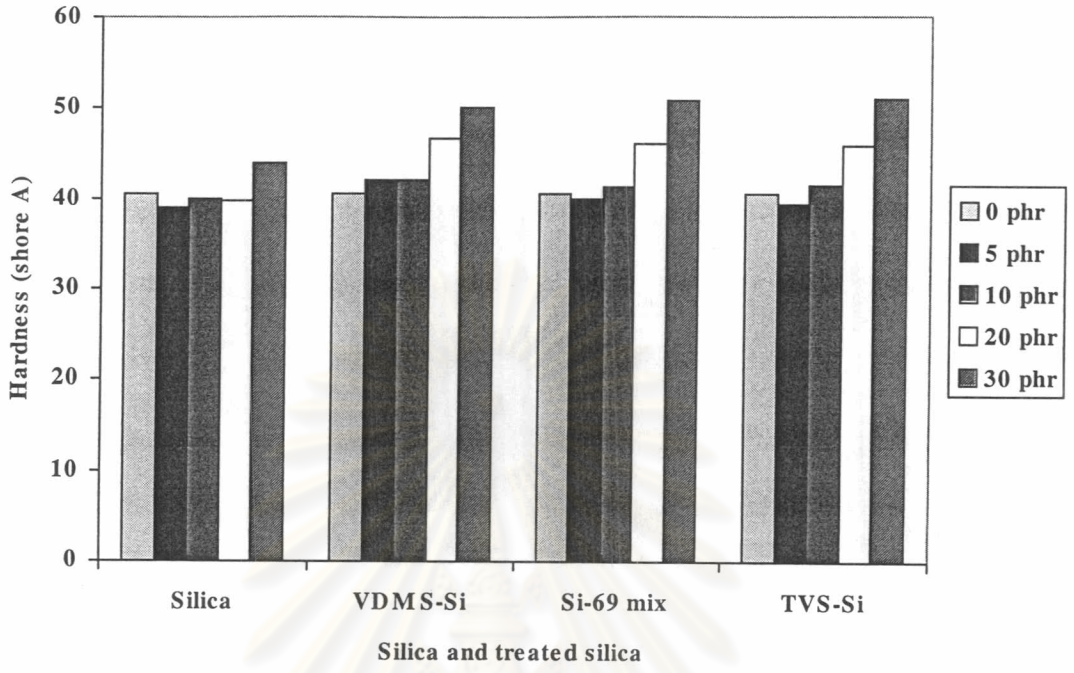


**Figure 4.14** Hardness of natural rubber composites filled with silica.

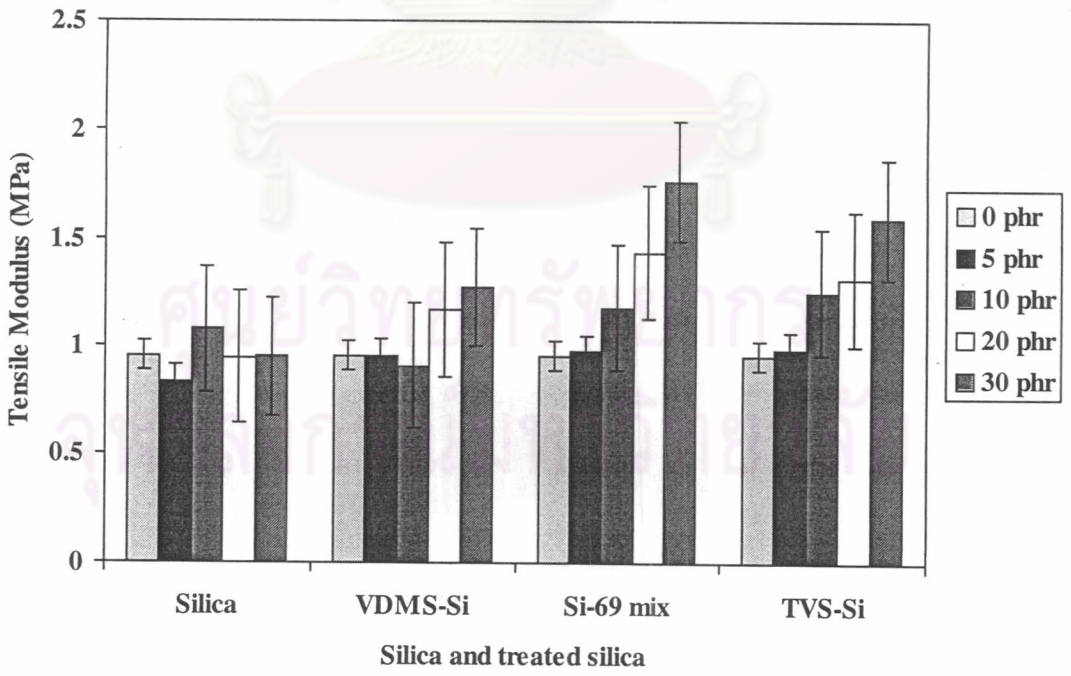


**Figure 4.15** Tensile modulus(M100) of natural rubber composites filled with silica.

### 4.3 Natural Rubber Composites Filled with VDMS-Si and Vulcanized in the Presence of Si-69

While VDMS-Si is a good filler due to its favorable curing characteristic (short cure time and scorch time), silica mixed with Si-69 render composites with superior tear strength and tensile modulus. Thus, a method of combining Si-69 with VDMS-Si for curing rubber composite was attempted. Curing behavior of composites filled with VDMS-Si, untreated silica mixed with Si-69 and VDMS-Si mixed with Si-69 are explained in terms of cure time, scorch time and Mooney viscosity as displayed in Figure 4.16, 4.17 and 4.18, respectively. Compared with the rubber composite filled with untreated silica and Si-69, the cure time of the rubber composites filled with VDMS-Si and Si-69 is lower at relatively high loading (20 and 30 phr). This can be regarded as an advantage of VDMS-Si incorporation. The curing process was accelerated by reactions between vinyl groups on the silica surface with rubber matrix and perhaps with Si-69. The presence of Si-69, however, extended the scorch time and raise Mooney viscosity.

As shown in Figure 4.19, tensile strength of rubber composites filled with VDMS-Si and Si-69 was slightly better than ones of rubber composites filled with untreated silica and Si-69 at low loading (5, 10 phr) indicating that vinyl groups on the silica surface helped strengthening the rubber composites. Meanwhile, the inferior tear strength of rubber composites filled with VDMS-Si at high loading were improved tremendously when Si-69 was added during curing (Figure 4.20). Figure 2.21 indicated that the combination method can slightly improve the hardness of composites in every filler loading. Most of all, the composites prepared by this

particular method showed the highest tensile modulus especially at low filler loading (5,10 phr).

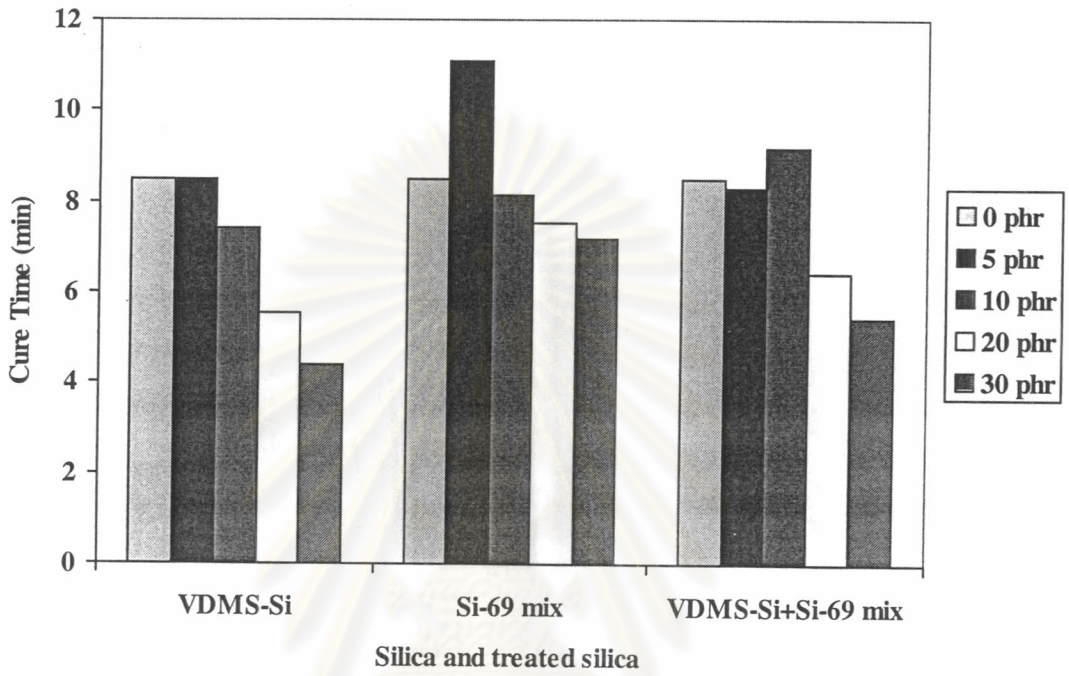


**Figure 4.16** Cure time ($t_{90}$) of rubber composites cured in the presence of Si-69.

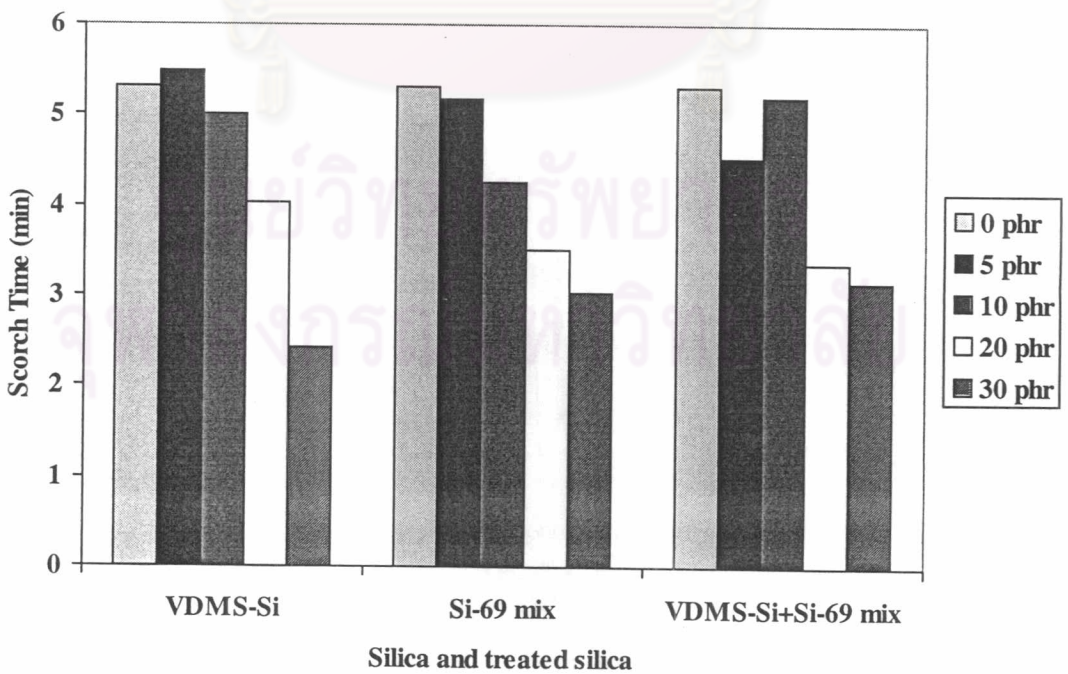


**Figure 4.17** Scorch time of natural rubber composites cured in the presence of Si-69.

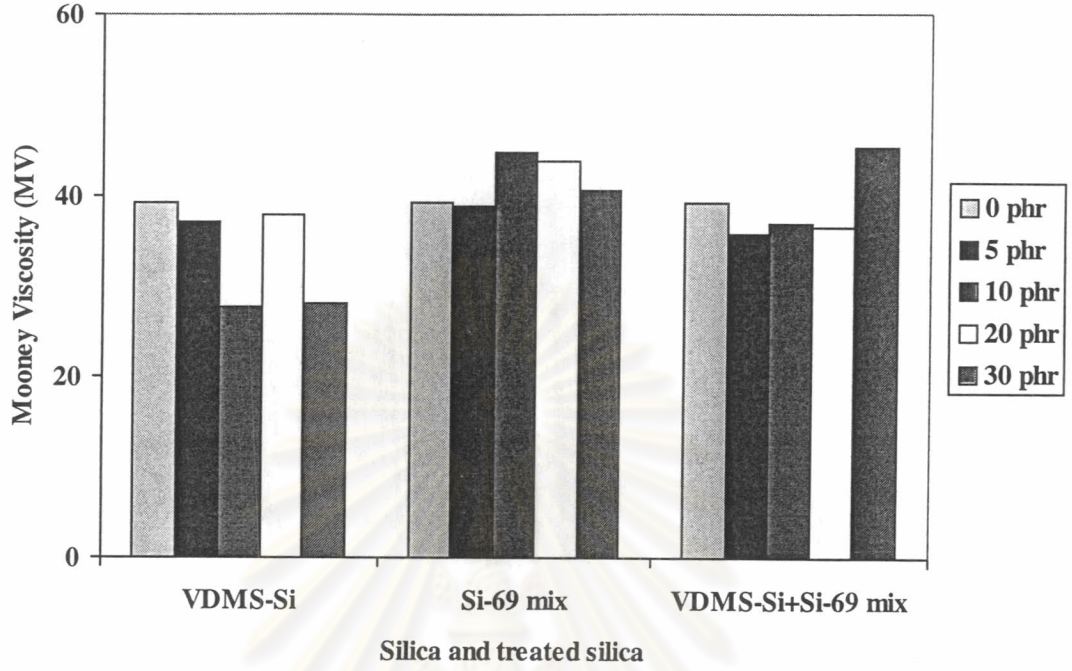


**Figure 4.18** Mooney viscosity of natural rubber composites cured in the presence of Si-69.

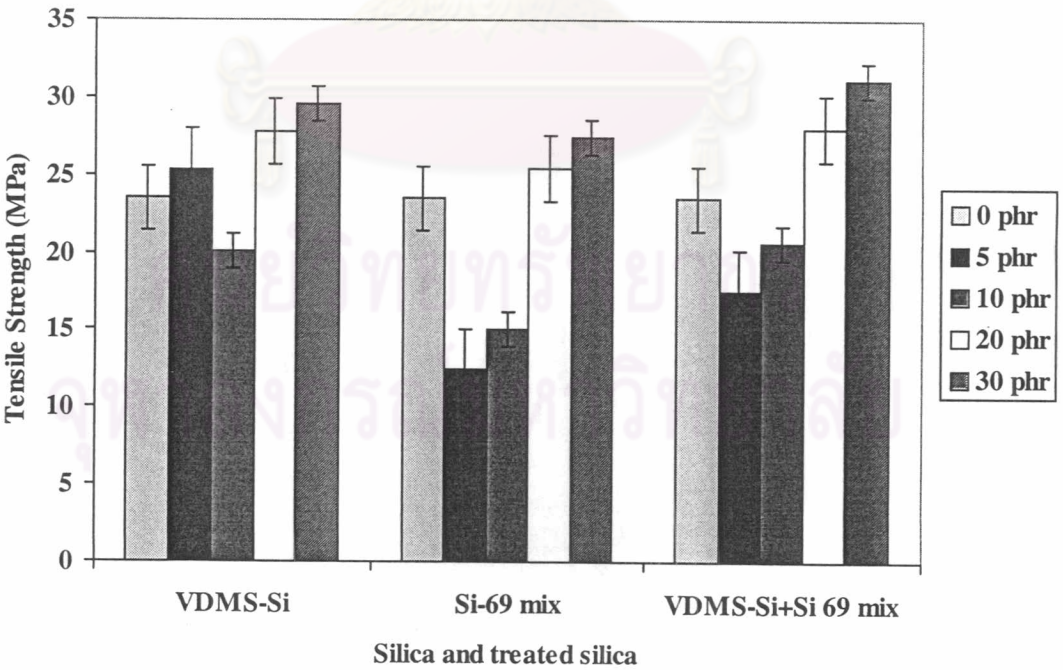


**Figure 4.19** Tensile strength of natural rubber composites cured in the presence of Si-69.

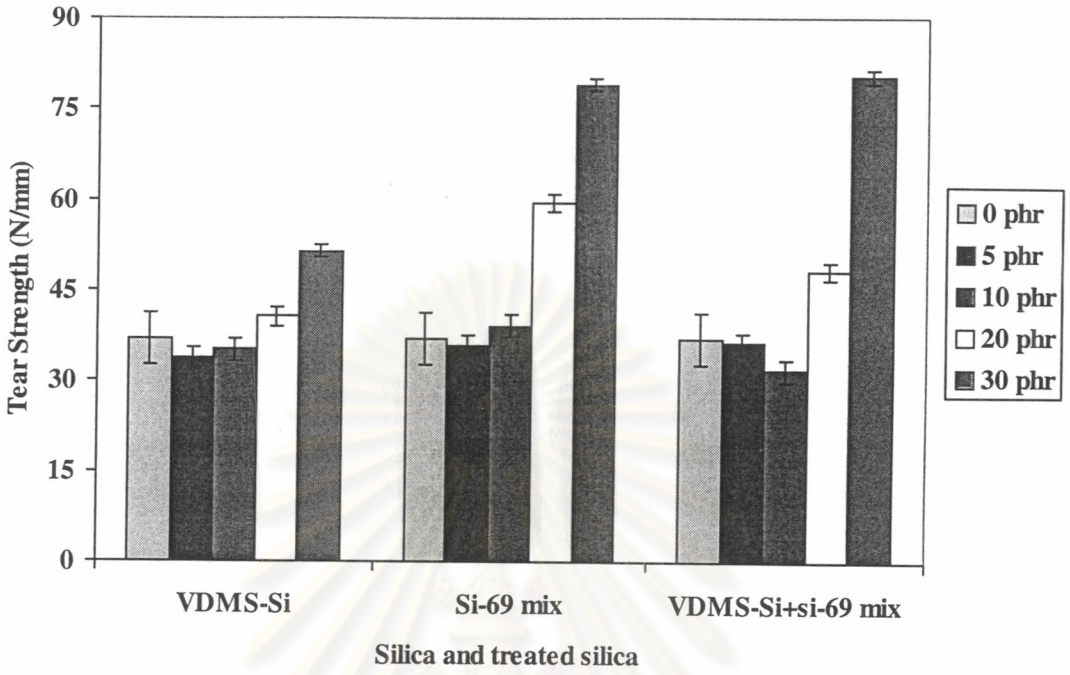


**Figure 4.20** Tear strength of natural rubber composites composites cured in the presence of Si-69.

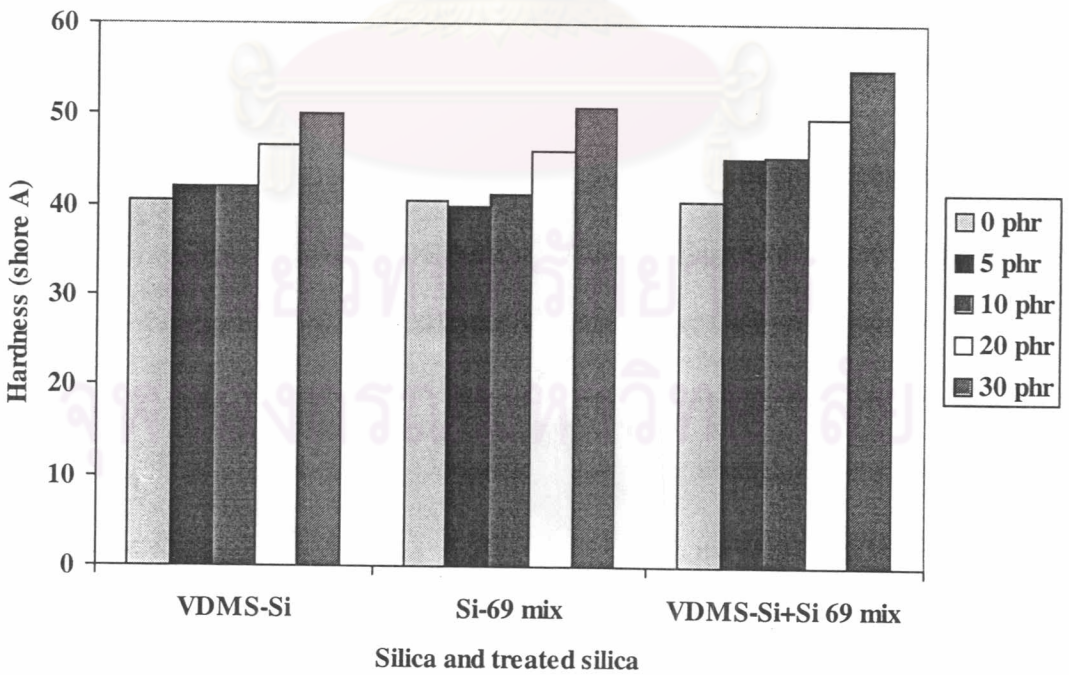


**Figure 4.21** Hardness of natural rubber composites cured in the presence of Si-69.

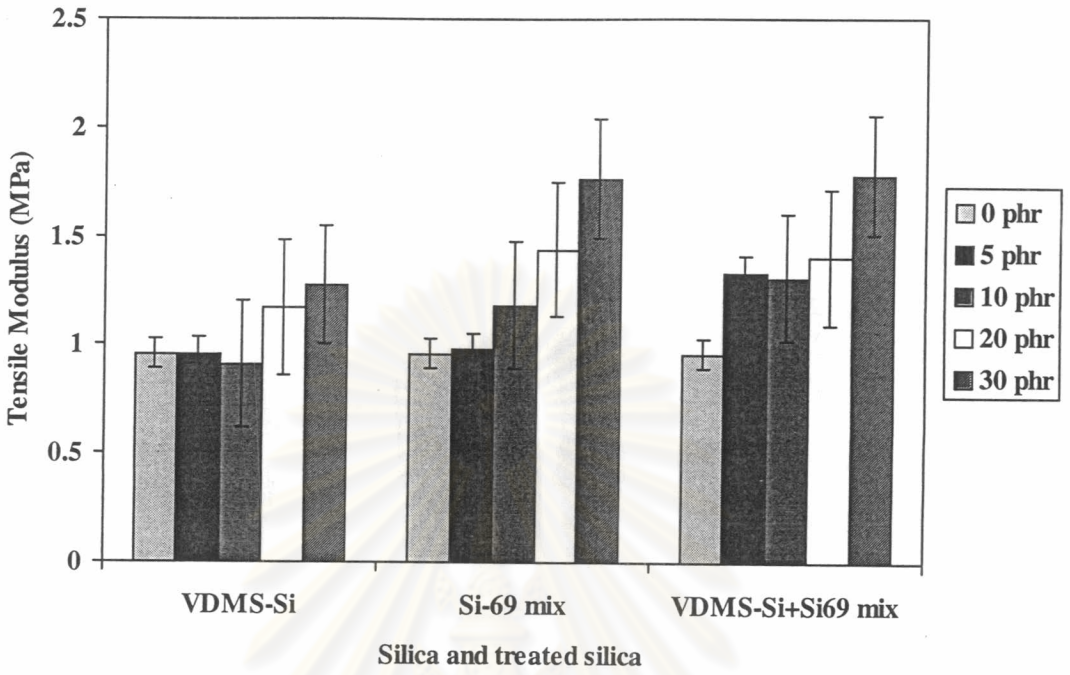


**Figure 4.22** Tensile Modulus (M100) of natural rubber composites cured in the presence of Si-69.

## 4.4 Determination of Silica Distribution in Natural Rubber Composites

A natural rubber composite without silica filler was first characterized. The analysis was done on four different areas of the same sample as shown in Figure 4.23. Topographic images and the corresponding mapping images of silica particle distribution are displayed on the left and right side, respectively. It can be seen that white spots scattering randomly on the topographic images do not represent the position of silica particles. The non-smooth surface is a result of freeze-fracture of the rubber composites during a sample preparation. On mapping images, white features occasionally appeared due to the silica contaminant existing in processing

machines ( i.e. two roll-mill, compression mold). The absence of silica in this set of sample can be verified by the elemental scan later shown in Figure 4.26.

Four sets of vulcanized rubber composites having 30 phr silica loading were chosen. Two representative topographic images along with the corresponding mapping images of each set of samples are illustrated in Figures 4.24-4.25. As similar to what has been discussed earlier, there is no specific correlation between the topography and the distribution of silica seen in the corresponding mapping image. Silica appeared as white particles homogeneously scatter on the surface. The dark area represented the natural rubber matrix without silica. The agglomeration appeared as large particulates was occasionally seen on all composites. The existence of silica was later confirmed by the elemental scan displayed in Figure 4.27. Similar feature of elemental scan was observed on all composites with approximately 8-12 % of silicon. There is no clear evidence indicating the difference of silica distribution between each composites. Thus, it can't be proven that an addition of VDMS-Si, TVS-Si or untreated silica with Si-69 really promotes the silica distribution based on the available information. Should the difference of silica distribution exist in the length scale smaller than what SEM analysis can probe, it is also impossible to distinguish the variation. An improvement in mechanical properties should then arise from chemical crosslinking at the interface between surface-treated silica and natural rubber.

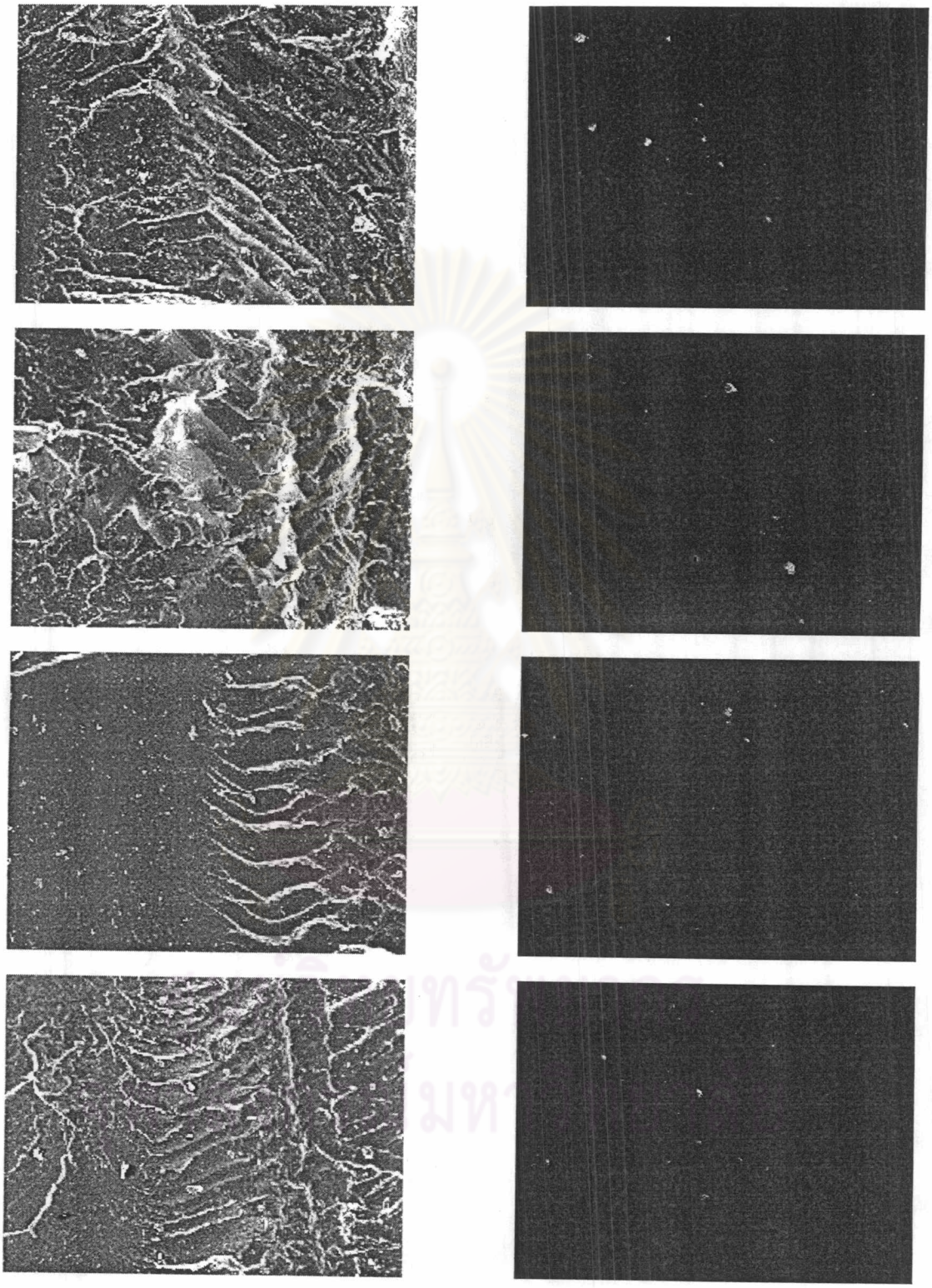

**Figure 4.23** SEM micrographs (left) and mapping images of silica particle distribution (right) of a natural rubber composite without silica.

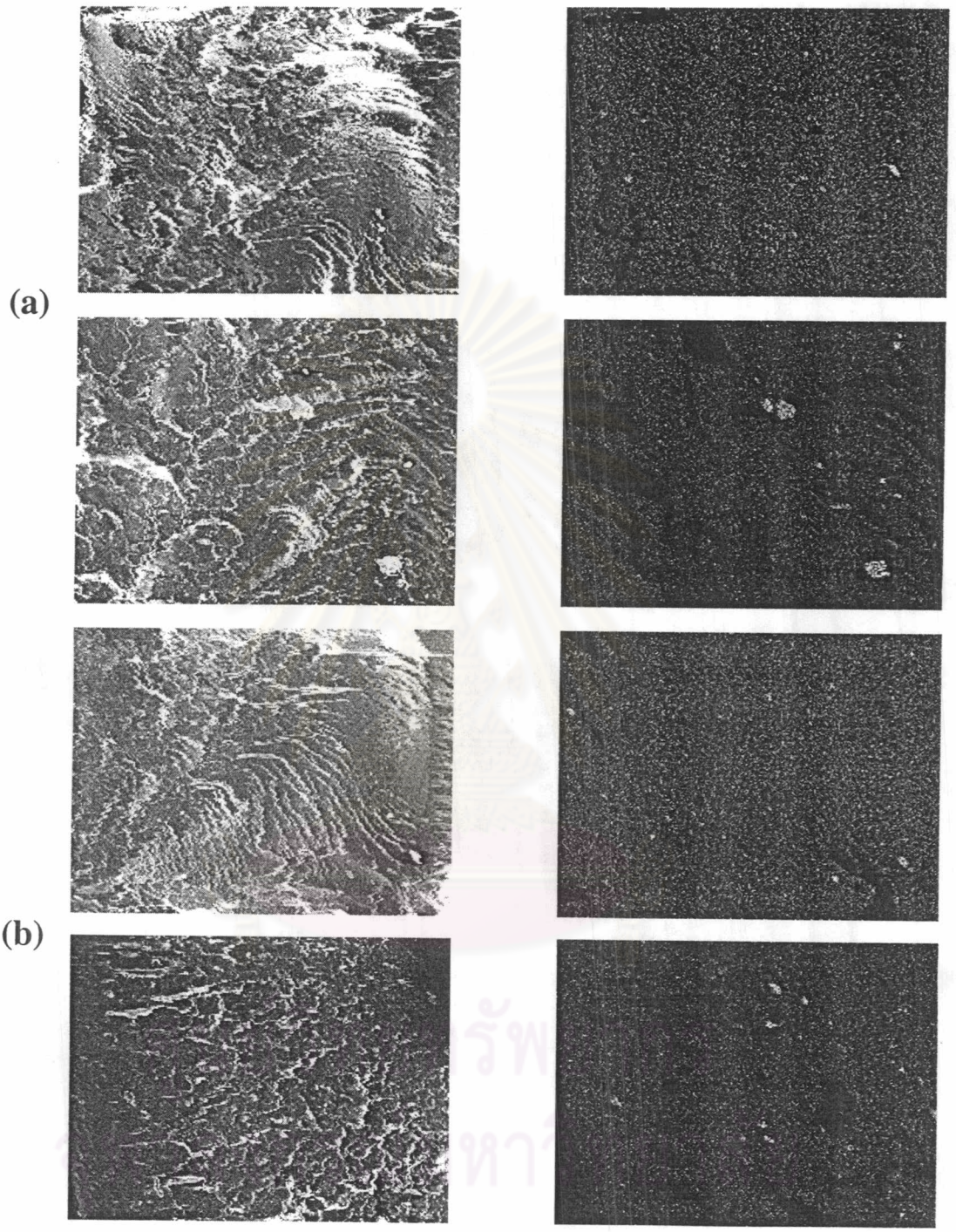


**Figure 4.24** SEM micrographs (left) and mapping images of silica particle distribution (right) of natural rubber composites containing (a) silica (b) silica mixed with Si-69.

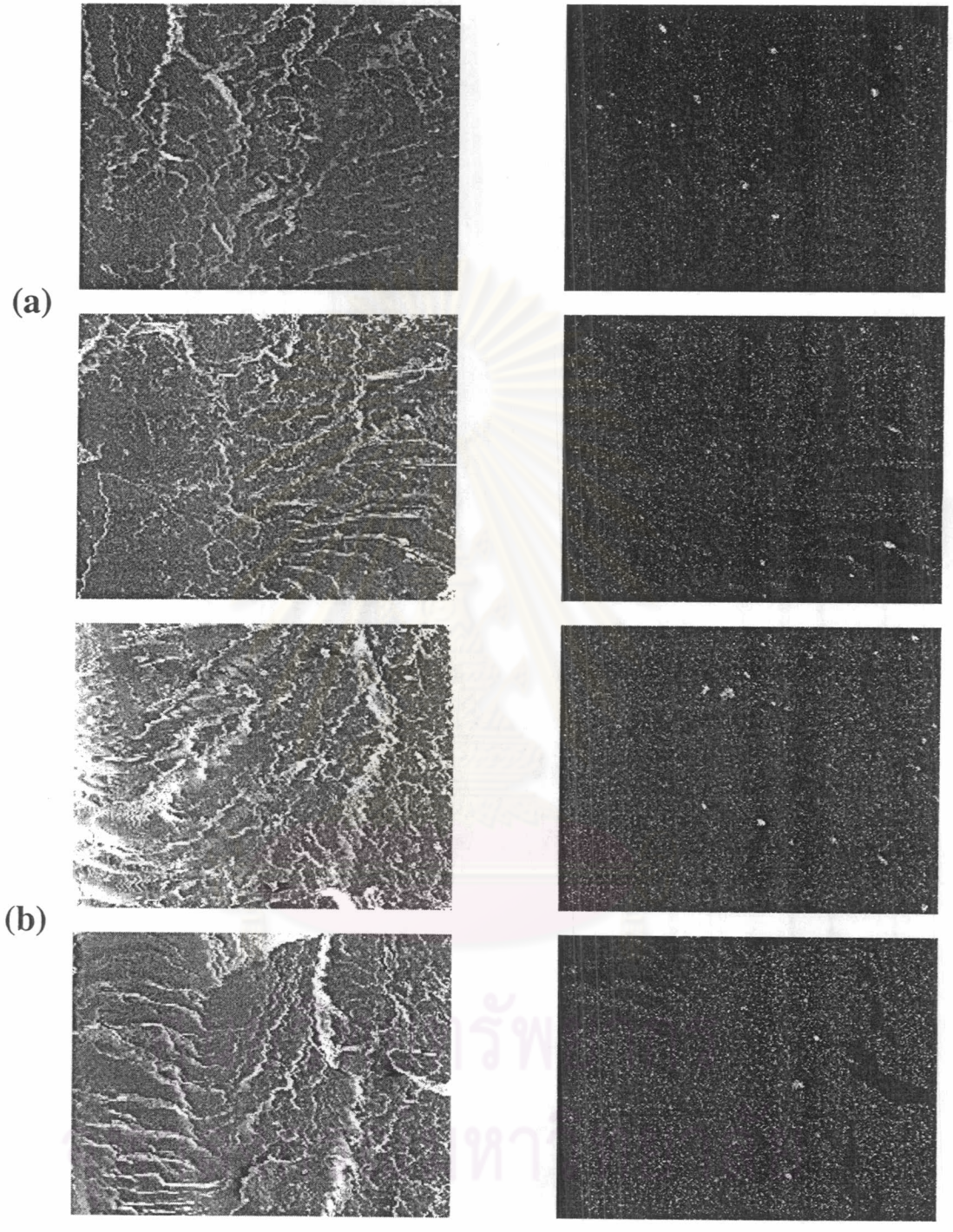


**Figure 4.25** SEM micrographs (left) and mapping images of silica particle distribution (right) of natural rubber composites containing (a) VDMS-Si (b) TVS-Si.

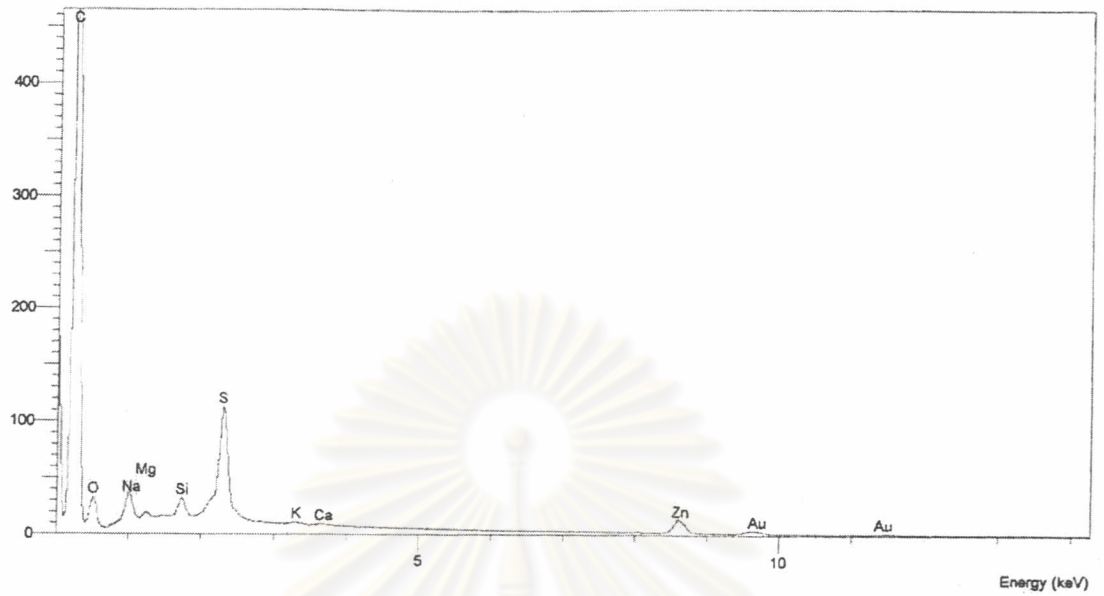


**Figure 4.26** An elemental scan on the surface of a natural rubber composite without silica.


**Figure 4.27** An elemental scan on the surface of a natural rubber composite filled with 30 phr VDMS-Si.